Available online at www.sciencedirect.com

ScienceDirect

IFAC PapersOnLine 56-2 (2023) 6549–6554

Thermal Images and Temperature Matrices for the State Assessment of Rolling Bearings

Edgar Daniel Gomez * **Giacomo Barbieri** *

* *Department of Mechanical Engineering, Universidad de los Andes, Bogotá, Colombia (e.mail: {ed.gomez10,g.barbieri}@uniandes.edu.co)*

Abstract: The assessment of the health state of rolling bearings is important for supporting the decision-making concerning their maintenance and operation. Even if different techniques and methods have been utilized, approaches based on Infrared Termography (IRT) have not been sufficiently explored. In this paper, the potential that IRT may have for classifying the severity of failures of rolling bearings is investigated. This study compares different approaches for analyzing thermal data woth the purpose of detecting outer-race defects in rolling bearings. Specifically, the study considers thermal-based analysis (TBA) using temperature matrices, intensity-based analysis (IBA) using thermal images, and combinations of these two methods. These approaches are evaluated based on their ability to classify the severity of the defects, building on promising results previously obtained in the field of Infrared Breast Thermography. An accuracy and F1-score exceeding 90% were achieved by combining the temperature matrix with the thermal image using pseudo colors and processing them with the VGG deep learning algorithm. These outcomes indicate the potential of IRT in assessing the condition of rolling bearings. It should be noted that while this work has explored the use of IRT for the classification of the health state of rolling bearings by running different operative conditions and taking thermal images from various angles and distances, further experiments are needed to fully validate the effectiveness of this approach.

Keywords: Prognostics and Health Management, Predictive Maintenance, Fault Diagnosis Assessment, State Assessment, Infrared Thermography, Deep Learning, Rolling Bearings.

1. INTRODUCTION

Prognostics and Health Management (PHM) is a preventive maintenance approach that aims to minimize unplanned downtime by using condition-based monitoring techniques. According to Li et al. (2020), PHM involves three main activities: fault diagnosis assessment, prognostic assessment, and health management. *Fault Diagnosis Assessment* (FDA) focuses on fault detection, isolation, and identification (Jardine et al., 2006). Additionally, the *State Assessment* (SA) activity is included in FDA, which aims to classify the severity of failures or the health state of the physical asset in case the failure has not yet occurred Li et al. (2020).

There are various techniques available for the SA of physical assets, including vibration and current monitoring, tribology, infrared thermography, and ultrasonic testing, among others. Wang and Gao (2006) state that *Infrared Thermography* (IRT) is a non-contact and non-invasive tool that can provide temperature distribution of a measured surface as a thermal image. IRT has been used for condition monitoring in different domains; see (Bagavathiappan et al., 2013). Although the use of IRT for the PHM of rotating machinery has been more limited (Lopez-Perez and Antonino-Daviu, 2017), this tool consists in an interesting option for condition monitoring due to the potential of this technology, together with the progressive decrease in the price of infrared cameras and the increase in their resolution (Hellier, 2001).

Effective *SA of rolling bearings* is crucial for enhancing the reliability and performance of rotating machinery, as bearing failures are one of the most common reasons for breakdowns. For instance, bearing failures can account for up to 44% of total faults in large induction motors (Zhang et al., 2010). Literature reviews on the SA of rolling bearings have been conducted by Cerrada et al. (2018) and El-Thalji and Jantunen (2015), where physics-based and data-driven models have been analyzed to identify degradation patterns related to health conditions. The reviews also discuss techniques and methods based on vibration, acoustic emission, current and voltage signals.

Several works can be found in the literature concerning the application of *IRT* for the *FDA of rolling bearings*. These works utilize both machine learning and deep learning techniques for the classification process.

Concerning *machine learning (ML)*, Younus and Yang (2012) present an intelligent diagnosis system for the classification of different machine conditions. The proposed algorithm utilizes support vector machines (SVM) and linear discriminant analysis methods to differentiate between healthy, shaft misalignment, mass unbalance and bearing fault states. Janssens et al. (2015) propose an automatic fault detection system focusing on bearings of rotating

10.1016/j.ifacol.2023.10.305

machinery. Their system is able to classify different faults using random forest and a SVM classifier. In Choudhary et al. (2020), a SVM and a complex decision trees classifier are utilized for diagnosing different bearing faults in induction motors, namely, inner and outer race defects, and lack of lubrication.

Concerning *deep learning* (DL), Yongbo et al. (2020) develop a FDA method using Convolutional Neural Network (CNN). The classified faults include race defects on the bearings and shaft unbalanced conditions. Jia et al. (2019) utilize bag-of-visual-word and CNN for the classification of faults of rolling bearings. Janssens et al. (2017) propose the use of transfer learning with a pre-trained VGG deep learning algorithm (Simonyan and Zisserman, 2014). Choudhary et al. (2021) compare the performance of a LeNet-5 CNN architecture and Adversarial Neural Network in the classification of six different fault types.

It can be noticed that the papers mentioned above only focus on fault detection and identification and do not address the *SA of rolling bearings*. However, in the recent study by Roldan et al. (2021), the potential of IRT for this purpose was investigated. The authors analyzed the ability of temperature indicators obtained from IRT images to classify the severity of failures in the outer-race of rolling bearings. Results showed that IRT has promising potential for the SA of rolling bearings as several indicators demonstrated a monotonic trend with respect to the severity of the failure.

The present study aims to further investigate the potential of IRT in the SA of rolling bearings. In order to reach this objective, we took inspiration from the *Infrared Breast Thermography* domain (Golestani et al., 2014): a method for the early detection of breast temperature anomalies related to breast cancer. In particular, Gogoi et al. (2019) compared thermal based analysis (TBA) using temperature matrices, and intensity based analysis (IBA) using thermal images for the classification of thermogram analyses exams. The best results were obtained by combining features from TBA and IBA with an accuracy of 83.22%.

IRT cameras acquire *thermal images* that can be converted into *temperature matrices* in which a temperature value is associated to each pixel (Jeffali et al., 2019); see Figure 1. Temperature matrices are analyzed through TBA methods, while thermal images through IBA methods. Given the promising results obtained in Golestani et al. (2014), in this paper TBA, IBA and different approaches for combining the two methods are compared in the classification of the severity of outer-race defects of rolling bearings. The paper is structured as follows: the utilized experimental setup is illustrated in section 2. Section 3 shows the comparison of TBA, IBA and their combination for the SA of rolling bearings. Obtained results are discussed in section 4 and finally, section 5 presents the conclusions and sets the directions for future work.

2. EXPERIMENTAL SETUP

The details of the utilized experimental setup can be found in (Roldan et al., 2021). In this section, the main features are resumed, along with the differences with respect to the previous work.

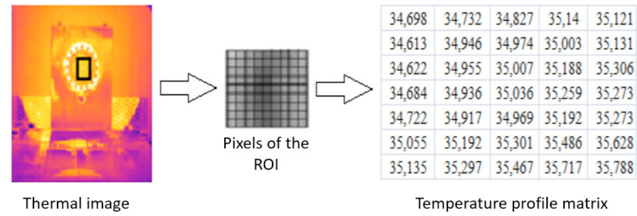

Fig. 1. Conversion of a thermal image into a temperature profile matrix. In the figure, ROI indicates the Region of Interest. The representation has been adopted from Jeffali et al. (2019)

To simulate the operation of faulty and healthy bearings, the *test bench* depicted in Figure 2 was utilized. The test bench comprises an induction motor, a flywheel, and three ball bearings. It enables the simulation of bearing failures, shaft misalignment, and unbalanced loads. In addition, by adjusting the frequency supplied to the motor, various operational conditions can be implemented.

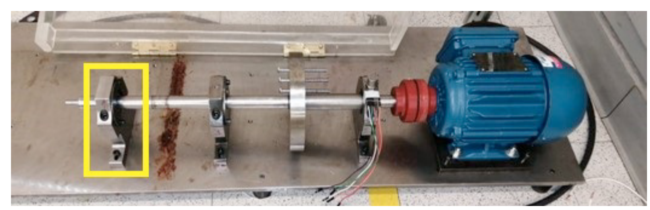

Fig. 2. Induction motor test bench utilized for the simulation of bearing failures. The tested bearing is indicated with a yellow rectangle.

To assess the indicators for the State Assessment (SA) of rolling bearings, *discrete faulty conditions* were created by introducing single point defects in the bearing outer-race using electrical discharge machining. A notch was incorporated in each bearing to establish three severity levels, with an approximate depth of 0.3mm and a width of 0.178mm (severity 1, S1), 0.356mm (severity 2, S2), and 0.533mm (severity 3, S3).

Our study involved the evaluation of the method robustness under different *operative conditions*, such as the supplied motor frequency of 20Hz, 40Hz, and 60Hz. Additionally, thermal images were captured from various *angles* and *distances* relative to the examined bearing, as shown in Figure 3, to simulate an industrial setting where the operator may manually capture the thermal images and may not be able to maintain consistent angles and distances.

During the experiment, the system began from a state of rest, and the temperature of the bearing under test was equal to the ambient temperature. As the system was set in motion, a transient behavior was observed before the steady-state temperature was reached. Consequently, it was necessary to determine the duration of the transient behavior and the appropriate acquisition frequency. To achieve this, a specific test was conducted. The temperature dynamics was modeled as a first-order system and the average time constant (τ) resulted in 35 min; see (Roldan et al., 2021) for the details of the mathematical model. The transient behaviour was quantified in 105 minutes, corresponding to three times the time constant. With respect to the *sampling frequency*, we decided to take one

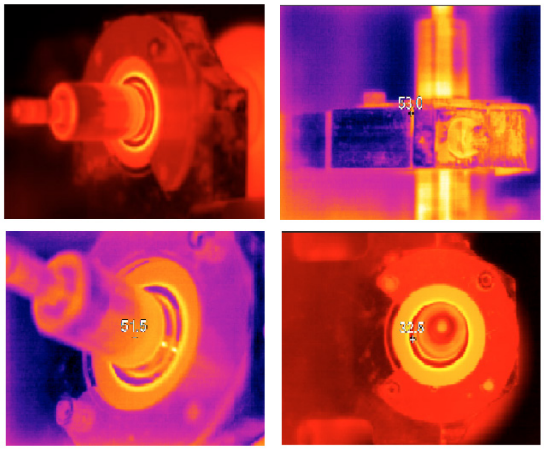

Fig. 3. IRT data collected at different points of view ranging from 0 to 90 degrees relative to the housing, and from below and above the test bench.

image each 5 minutes. This value corresponds to 7 times the system time constant, enabling the acquisition of the transient behavior.

A *data set* of 2640 IRT data was acquired. Each IRT datum consists of a thermal image and the corresponding temperature matrix. A resolution of 480 × 640 pixels was obtained for the thermal images and matrices of 240 × 321 elements for the temperature matrices. Data were acquired both for the healthy state and the three severity levels of failures before indicated. The number of data for each state is shown in Table 1. Assuming that the steady state is reached after 105 minutes, experiments were performed for 175 minutes to grant both the acquisition of the transient and steady-state behaviour.

Table 1. Data acquired for the healthy state (S0) and the three severity levels of failures.

Severity level			
S0	S1	S2	S3
619	623	670	728
23.4%	23.6%	25.4%	27.6%

3. TBA, IBA AND MIXED APPROACHES

In this section, TBA, IBA and mixed approaches that combine thermal images and temperature matrices are illustrated.

In a preliminary study on TBA, a multi-class support vector machine (SVM) was trained to classify the severity of the bearing failures. A region of interest containing the bearing was selected in the temperature matrix and first-order statistical indicators – such as mean, standard deviation, kurtosis, and energy – were computed as features. Then, principal component analysis was applied to train the SVM. However, results were not promising since an accuracy over the test set of 34% and an F1-score of 51% were obtained. Consequently, given the low performance DL methods were utilized showing more promising results.

Given the above, section 3.1 illustrates the DL algorithms utilized to compare the TBA, IBA and mixed approaches, section 3.2 the methods utilized for the TBA and IBA analyses and section 3.3 the alternatives investigated for the combination of TBA and IBA.

3.1 Deep learning methods

Two DL algorithms were selected to compare the approaches based on TBA, IBA, and their combination: i) EfficientNet scaling strategy (Tan and Le, 2019): a methodology that exhibited high accuracy results on ImageNet classification with a significant reduction in the number of involved parameters with respect to CNN; ii) VGG ConNet (Simonyan and Zisserman, 2014): an architecture proposed in image recognition to investigate the effects of the network depth on the obtained accuracy. In particular, TBA, IBA, and their combination were compared based on EfficienNet-b0,b3,b7, and VGG-16, 19. Both EfficienNet and VGG work with an optimal resolution of 224 x 224 pixels. Therefore, a rescaling of both thermal images and temperature matrices was necessary. Next, the two methods are briefly resumed.

EfficienNet Tan and Le (2019) studied model scaling and proposed a methodology to uniformly scale the width (number of channels), the depth (number of layers), and the resolution (input image size) of CNN to achieve better performance. Using the neural architecture, they designed a new network and scale it up obtaining a family of networks: from EfficientNet-b0 to EfficientNet-b7, named in increasing accuracy and parameters.

For scaling the dimensions, they proposed three coefficients – α, β and γ – and a compound coefficient ϕ that scales the network as follows:

$$
\begin{aligned}
depth &: d = \alpha^{\phi} \\
width &: w = \beta^{\phi} \\
resolution &: r = \gamma^{\phi} \\
s.t. \quad & \alpha \cdot \beta^2 \cdot \gamma^2 \approx= 2
\end{aligned}
$$

The dimension parameters are determined by grid search, while ϕ depends on the computational resources available for the scaling of the model. Authors started their experimentation with EfficientNet-b0 and changed the parameters until reaching the highest classification accuracy of 84.3% on the image database ImageNet. This was possible by using 66 million parameters on EfficientNet-b7.

As part of EfficientNet backbone, authors applied two main methodologies that increased the obtained performance. As building block of the network, an inverted residual structure from MobileNetV2 was used (Sandler et al., 2018). Furthermore, squeeze and excitation units were implemented as part of inverted residual blocks to assess the channel prioritization considering the inter dependencies (Hu et al., 2018).

VGG In VGG, Simonyan and Zisserman (2014) explored the effect of depth on the accuracy of the CNN architectures. Based on AlexNet, convolutional layers were added while fixing parameters such as input resolution of 224 x 224 pixels. Their convolutional block was designed with a small receptive field of 3 x 3 kernels and a stride and padding of 1 in order to preserve the spatial resolution.

Five max pooling were added after some convolutional layers with a 2 x 2 pixel window and a stride of 2.

On ImageNet, they began the experimentation with a width of 64 channels and increased them by a factor of 2 after each max-pooling layer. The process was repeated until 512 channels were reached. VGG of different depths were tested ranging from 11 to 19 layers. However, VGG16 and VGG19 are the most popular and highest-performance architectures and were utilized in this work.

3.2 TBA and IBA analyses

In TBA, temperature matrices are provided to the DL algorithm as shown in the top part of Figure 4. The networks have been trained during 40 epoch of batch size 10, with a learning rate of $1 * 10^4$ and an Adam optimizer. In accordance with (Tan and Le, 2019), SiLU (Sigmoid Linear Units) was used as an activation function and stochastic depth was applied for EfficientNet. In VGG models, ReLU (Rectifier Linear Units) was adopted as an activation function in accordance with (Simonyan and Zisserman, 2014). Cross-entropy loss was utilized as a proper loss function for classification tasks. A resizing was applied to the temperature matrices in order to account for the optimal 224 x 224 input resolution of EfficientNet and VGG.

The same approach was utilized for the IBA analysis as shown in the bottom part of Figure 4; i.e. 40 epochs, batch size of 10, the learning rate of $1*10^4$, and Adam optimizer. Equally, SiLU and stochastic depth were applied for EfficientNet and ReLU for VGG with cross entropy as a loss function.

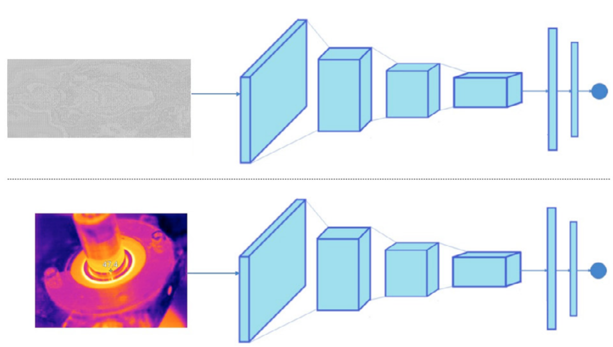

Fig. 4. TBA analysis is reported in the top part of the figure, while IBA analysis on the bottom part.

3.3 Mixed approaches

Inspired by the methodology proposed by (Yala et al., 2019) for breast cancer prediction with mammography data, a mixed approach that combines TBA and IBA analyses is proposed. Feeding a DL algorithm with both types of data can improve feature learning and provide additional insights to enhance pattern recognition and subsequent classification. The combination of TBA and IBA can occur in different ways. In this work, the three methods shown in Figure 5 are tested:

- *4-channel*: this method proposes the concatenation of the temperature matrix to the thermal image through pseudo colors. Then, the resulting 4-channel matrix is fed into the baselines for the classification;
- *Feature vector*: another possible approach is to extract a feature vector from the temperature matrix. Thermal images are fed to the convolutional backbone of the model and then, the temperature feature vector is concatenated to the flattened output of the convolutional layers; i.e. as input of the linear layers utilized for the classification. The feature vector is made of first-order statistical indicators: mean, median, standard deviation, minimum value, and maximum value;
- *4-fvector*: a third approach consists of the combination of the previous ones. Here, a 4-channel matrix made of the temperature matrix and the thermal image is fed into the convolutional backbone, and a feature vector extracted from the temperature matrix is concatenated to the flattened output of the convolutional layers; i.e. as input of the linear layers utilized for the classification.

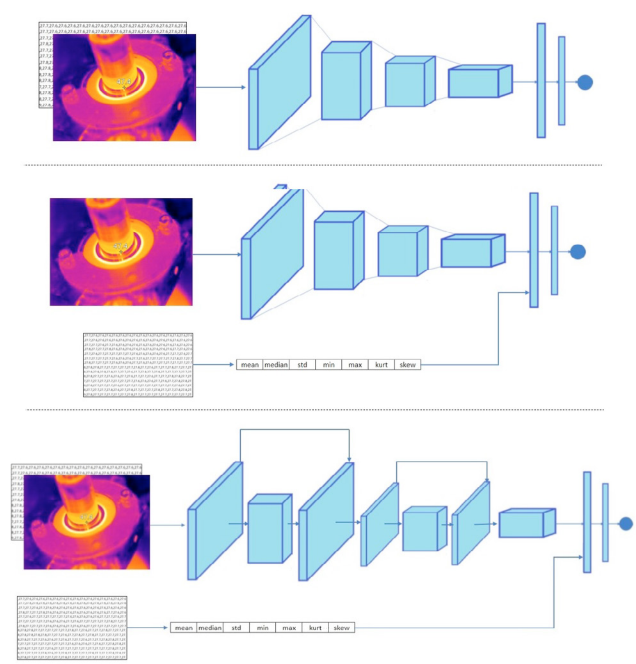

Fig. 5. Methods proposed for the combination of hybrid approaches. The 4-channel method is reported on the top part of the image, the feature vector on the middle part and 4-fvector on the bottom part.

4. RESULTS AND DISCUSSION

In this section, the comparison among TBA, IBA and the mixed approaches is performed. For this, the data set shown in Table 1 was split into training, validation, and test data of respectively 2138 (81%), 238 (9%) and 264 (10%) elements. Each datum was annotated with the corresponding bearing state. Then, the DL algorithms presented in section 3.1 were trained on the data set following the methods described in section 3.2 and section 3.3. Different inputs were provided to the algorithms based on the studied approach; i.e. temperature matrices for TBA analysis, thermal images for IBA analysis, and both data for the mixed approaches. During training, validation, and testing, data augmentation was applied to add modified copies of the elements of the data set with the objective to increase the feature learning potential of the DL approaches.

Table 2 and Table 3 respectively report the *accuracy* and *F1-score* obtained with the different approaches and the tested DL algorithms. The accuracy quantifies the correct predictions among the total number of classified data points, while the F1-score leverages precision and recall in a single harmonic mean of these two quantities. In a perfect classifier, both metrics should be 1.0. Some experiments with EfficientNet-b7 were not performed since it would have required high computational resources without a substantial improvement in the classification performance.

Table 2 and Table 3 indicate that the mixed approaches generally reach better results than TBA and IBA. In particular, the *4-channel mixed approach* had the best performance due to its ability to identify the healthy state of rolling bearings with reduced false positives and false negatives as shown in the confusion matrix of Figure 6. In accordance with the investigation of (Gogoi et al., 2019) in the infrared breast cancer domain, the obtained results shown that the combination of features from TBA and IBA improves the representational power of the classification model also for the state assessment of rolling bearings.

Furthermore, *VGG* resulted the most promising architecture having the best performance among the investigated approaches. Nevertheless, due to the increased number of parameters of VGG compared to EfficientNet, EfficientNet-b3 backbone may be utilized when computational resources constitute a limitation. In fact, the algorithm results in a good ratio between performance and number of parameters.

Finally, it can be noticed that accuracy and F1-score of about 90% were obtained. It is worth mentioning that different operative conditions have been run (i.e. supplied motor frequency of 20Hz, 40Hz and 60Hz) and that thermal images have been taken at different angles and distances from the studied bearing. Therefore, IRT seems a promising tool for the *state assessment of rolling bearings*.

Fig. 6. Confusion matrix for the 4-channel method.

5. CONCLUSION AND FUTURE WORK

The use of infrared thermography for the state assessment of rolling bearings is a promising technique that has not been extensively investigated. Given the high percentage of faults caused by rolling bearings, the application of this technique could provide significant benefits in terms of improving the reliability and performance of rotating machinery. While there are various approaches and methods available for the assessment of rolling bearings, the potential of *Infrared Thermography* for this purpose needs further exploration.

The aim of this research was to investigate the possibility of using IRT to categorize the *severity of failures* in the outer-race of rolling bearings. To achieve this, the study involved the creation of various single point defects on the bearing outer-race using electrical discharge machining, and thermal images were taken while the bearings were in operation. A comparison was performed between thermal based analysis (TBA) using temperature matrices, intensity based analysis (IBA) using thermal images and mixed approaches that utilize both types of data. Furthermore, TBA, IBA and mixed approaches were compared with EfficienNet and VGG DL algorithms. An accuracy and F1-score exceeding 90% were achieved by combining the temperature matrix with the thermal image using pseudo colors and processing them with the VGG deep learning algorithm. These outcomes indicate the potential of IRT in assessing the condition of rolling bearings.

This work focused on a data set recorded over a single test bed and the same type of rolling bearing. Therefore, *future works* should be directed toward defining a broader data set and the establishment of a new benchmark. Next, two research opportunities are presented:

- *Industrial validation*: even if thermal images were taken at different angles and distances from the studied bearing, the effects of further noises — typical of industrial workplaces — should be investigated; e.g. variations in environmental temperature, dust, light, and emissivity amonsts others.
- *Non-IRT approaches*: IRT needs to be compared with vibration and acoustic techniques to fully assess its potential on the state assessment of rolling bearings.

REFERENCES

Bagavathiappan, S., Lahiri, B., Saravanan, T., Philip, J., and Jayakumar, T. (2013). Infrared thermography for condition monitoring–a review. *Infrared Physics & Technology*, 60, 35–55.

Cerrada, M., Sánchez, R.V., Li, C., Pacheco, F., Cabrera, D., de Oliveira, J.V., and Vásquez, R.E. (2018). A review on data-driven fault severity assessment in rolling bearings. *Mechanical Systems and Signal Processing*, 99, 169–196.

Choudhary, A., Goyal, D., and Letha, S.S. (2020). Infrared thermography-based fault diagnosis of induction motor bearings using machine learning. *IEEE Sensors Journal*, 21(2), 1727–1734.

Choudhary, A., Mian, T., and Fatima, S. (2021). Convolutional neural network based bearing fault diagnosis of rotating machine using thermal images. *Measurement*, 176, 109196.

Table 2. Comparison of the accuracy obtained with the TBA, IBA, and combined approaches with the EfficientNet and VGG backbones.

	EfficientNet-b0	**EfficientNet-b3**	**EfficientNet-b7**	**VGG16**	**VGG19**
TBA	75.38%	79.55%	79.17%	86.36%	87.12%
IBA	73.55%	74.24%	79.55%	89.39%	88.26%
4-channel	78.41%	83.33%	76.14%	90.91%	91.29%
Feature vector	74.24%	77.65%	N/A	89.89%	85.23%
4-fvector	71.59%	76.14%	N/A	89.39%	82.95%

Table 3. Comparison of the F1-score obtained with the TBA, IBA, and combined approaches with the EfficientNet and VGG backbones.

	EfficientNet-b0	**EfficientNet-b3**	**EfficientNet-b7**	**VGG16**	**VGG19**
TBA	75.78%	79.89%	79.50%	86.58%	87.30%
IBA	73.66%	74.18%	79.79%	89.39%	89.49%
4-channel	78.34%	83.61%	76.20%	90.95%	91.28%
Feature vector	74.19%	77.58%	N/A	89.41%	85.34%
4-fvector	71.61%	76.28%	N/A	89.64%	83.12%

El-Thalji, I. and Jantunen, E. (2015). A summary of fault modelling and predictive health monitoring of rolling element bearings. *Mechanical systems and signal processing*, 60, 252–272.

Gogoi, U.R., Majumdar, G., Bhowmik, M.K., and Ghosh, A.K. (2019). Evaluating the efficiency of infrared breast thermography for early breast cancer risk prediction in asymptomatic population. *Infrared Physics & Technology*, 99, 201–211.

Golestani, N., EtehadTavakol, M., and Ng, E. (2014). Level set method for segmentation of infrared breast thermograms. *EXCLI journal*, 13, 241.

Hellier, C. (2001). *Handbook of nondestructive evaluation*. McGraw-Hill Professional.

Hu, J., Shen, L., and Sun, G. (2018). Squeeze-and-excitation networks. In *Proceedings of the IEEE conference on computer vision and pattern recognition*, 7132–7141.

Janssens, O., Schulz, R., Slavkovikj, V., Stockman, K., Loccufier, M., Van de Walle, R., and Van Hoecke, S. (2015). Thermal image based fault diagnosis for rotating machinery. *Infrared Physics & Technology*, 73, 78–87.

Janssens, O., Van de Walle, R., Loccufier, M., and Van Hoecke, S. (2017). Deep learning for infrared thermal image based machine health monitoring. *IEEE/ASME Transactions on Mechatronics*, 23(1), 151–159.

Jardine, A.K., Lin, D., and Banjevic, D. (2006). A review on machinery diagnostics and prognostics implementing condition-based maintenance. *Mechanical systems and signal processing*, 20(7), 1483–1510.

Jeffali, F., Ouariach, A., El Kihel, B., and Nougaoui, A. (2019). Diagnosis of three-phase induction motor and the impact on the kinematic chain using non-destructive technique of infrared thermography. *Infrared Physics & Technology*, 102, 102970.

Jia, Z., Liu, Z., Vong, C.M., and Pecht, M. (2019). A rotating machinery fault diagnosis method based on feature learning of thermal images. *Ieee Access*, 7, 12348–12359.

Li, R., Verhagen, W.J., and Curran, R. (2020). A systematic methodology for Prognostic and Health Management system architecture definition. *Reliability Engineering and System Safety*, 193.

Lopez-Perez, D. and Antonino-Daviu, J. (2017). Application of infrared thermography to failure detection in industrial induction motors: case stories. *IEEE Transactions on Industry Applications*, 53(3), 1901–1908.

Roldan, S., Sanchez-Londono, D., and Barbieri, G. (2021). Thermographic indicators for the state assessment of rolling bearings. *IFAC-PapersOnLine*, 54(1), 1218–1223.

Sandler, M., Howard, A., Zhu, M., Zhmoginov, A., and Chen, L.C. (2018). Mobilenetv2: Inverted residuals and linear bottlenecks. In *Proceedings of the IEEE conference on computer vision and pattern recognition*, 4510–4520.

Simonyan, K. and Zisserman, A. (2014). Very deep convolutional networks for large-scale image recognition. *arXiv preprint arXiv:1409.1556*.

Tan, M. and Le, Q. (2019). Efficientnet: Rethinking model scaling for convolutional neural networks. In *International conference on machine learning*, 6105–6114. PMLR.

Wang, L. and Gao, R.X. (2006). *Condition monitoring and control for intelligent manufacturing*. Springer Science & Business Media.

Yala, A., Lehman, C., Schuster, T., Portnoi, T., and Barzilay, R. (2019). A deep learning mammography-based model for improved breast cancer risk prediction. *Radiology*, 292(1), 60–66.

Yongbo, L., Xiaoqiang, D., Fangyi, W., Xianzhi, W., and Huangchao, Y. (2020). Rotating machinery fault diagnosis based on convolutional neural network and infrared thermal imaging. *Chinese Journal of Aeronautics*, 33(2), 427–438.

Younus, A.M. and Yang, B.S. (2012). Intelligent fault diagnosis of rotating machinery using infrared thermal image. *Expert Systems with Applications*, 39(2), 2082–2091.

Zhang, P., Du, Y., Habetler, T.G., and Lu, B. (2010). A survey of condition monitoring and protection methods for medium-voltage induction motors. *IEEE Transactions on Industry Applications*, 47(1), 34–46.